Significance of Cell Size and Tissue Structure in Electrical Trauma

D. C. GAYLOR, K. PRAKAH-ASANTE AND R. C. LEE

The Laboratory for Electromagnetic and Electronic Systems, the Energy Laboratory, and the Harvard-M.I.T. Division of Health Sciences and Technology, Massachusetts Institute of Technology, 77 Massachusetts Ave., Cambridge, Massachusetts U.S.A.

High-voltage electrical trauma frequently leads to extensive and selective destruction of muscle and nerve tissue. In this paper, the mechanism of plasma membrane disruption due to the large transmembrane potentials imposed during electrical trauma is used to explain the particular susceptibility of muscle and nerve cells to damage. It is proposed that this vulnerability is partially due to the relatively large size of these cells. A distributed-parameter electric cable model of an elongated cell is used to examine the alteration of the transmembrane potential caused by a 60 Hz electric field applied parallel to the long axis of the cell. The maximum predicted transmembrane potential occurs at the ends of the cell and is strongly cell-size dependent. Theories are discussed which illustrate how this could explain the predisposition of skeletal muscle to cell membrane breakdown and rupture. The predicted effect of either close-neighboring cells in a tissue or cell contact with cortical bone is even greater induced transmembrane potentials and increased probability of rupture. This is the first hypothesis which explains the clinically-observed pattern of tissue damage resulting from electrical trauma.

Introduction

Major electrical trauma produces a spectrum of tissue injuries which range from the obvious thermal destruction of tissue at the current entry and exit points to the gradual onset of neurologic defects in the absence of apparent thermal injury (Sances *et al.*, 1979; Farrell & Starr, 1968). Skeletal muscle and nerve cells seem most susceptible to electrical injury. Many of the immediate clinical signs of electrical injury relate to neuromuscular damage. Intense muscular spasm and rigor are often described by witnesses, and are frequent presenting signs at hospital admission (Jaffe, 1928). Extensive muscle injury is so common that reported major limb amputation rates of 65% are not unusual (Butler & Gant, 1977).

Joule heating is widely believed to mediate the underlying cellular injury during electrical trauma. However, not all clinical manifestations are readily explained in this way, in particular the increased susceptibility of larger cells, such as skeletal muscle cells and nerve cells, to damage. While fundamental studies on the mechanisms of thermal injury to cells do not suggest that larger cells are more vulnerable to thermal injury than smaller cell types (Moritz & Henriques, 1947; Moussa *et al.*, 1979), substantial theoretical evidence exists which suggests that these cells are more

© 1988 Academic Press Limited

vulnerable to plasma membrane rupture by electrical breakdown. The clinical evidence which suggests that muscle and nerve cell membrane rupture can occur in an electrical trauma includes the release of large quantities of myoglobin from the intracellular space (Baxter, 1970), and the elevated levels of arachidonic acid production, suggesting increased intracellular free calcium (Robson et al., 1983). In many instances of electrical trauma, the imposed electric field in the tissue is of sufficient magnitude to cause electrical breakdown of cell membranes and cell lysis (Lee & Kolodney, 1987).

In this paper, it is proposed that the relatively high susceptibility of skeletal muscle cells to electrical injury is related to their large size compared with the less frequently injured connective tissue cells. It is demonstrated analytically that skeletal muscle cells oriented parallel to an applied d.c. electric field are subjected to an induced transmembrane potential which is greatest in magnitude at the cell ends and increases in magnitude with increasing cell length and radius. Large cells can exhibit significantly higher transmembrane potentials than smaller cell types in the same field. This is consistent with the predictions for nerve cells in a field (Tranchina & Nicholson, 1986). When the cells are subjected to sinusoidal fields at the commercial power frequency of 60 Hz, the magnitude of the induced transmembrane potential is less than that induced by d.c. fields of the same amplitude. Furthermore, in a 60 Hz sinusoidal field, the effect of cell charging modes is observed as the induced transmembrane potential is calculated for cells of different lengths. It is observed that the induced transmembrane potential reaches a peak magnitude for cells of a specific size and is significantly less for smaller or larger cell lengths.

Theories are briefly discussed which link the probability of cell membrane rupture to the square of the induced transmembrane potential. Thus, the degree to which a muscle cell is vulnerable to membrane electrical breakdown and rupture is strongly cell-size dependent. Finally, when the effects of neighboring cells are considered, it is demonstrated that the maximum transmembrane potential increases with decreasing intercellular distance. The analysis can be interpreted to predict patterns of damage within a muscle based on the cell's immediate environment. As will be shown, it appears to explain the clinical observation that muscle cells adjacent to bone have the greatest vulnerability to damage in an electrical trauma, while those adjacent to the fascial planes have the least vulnerability.

Theory

Major electrical trauma frequently involves the upper extremity, setting up current pathways as suggested in Fig. 1. In such instances, the long axes of most of the skeletal muscle and large nerve cells are oriented in the direction of the electric field lines. Characteristically, at frequencies much less than 1 MHz, mammalian cell membranes are highly insulating compared with the intracellular and extracellular fluids. As a consequence, currents established by low-frequency fields in the extracellular space are diverted around the cells, leading to enhancement of the induced transmembrane potentials. For a non-spherical cell in an electric field, the maximum induced transmembrane potential will depend on the cell's orientation with respect
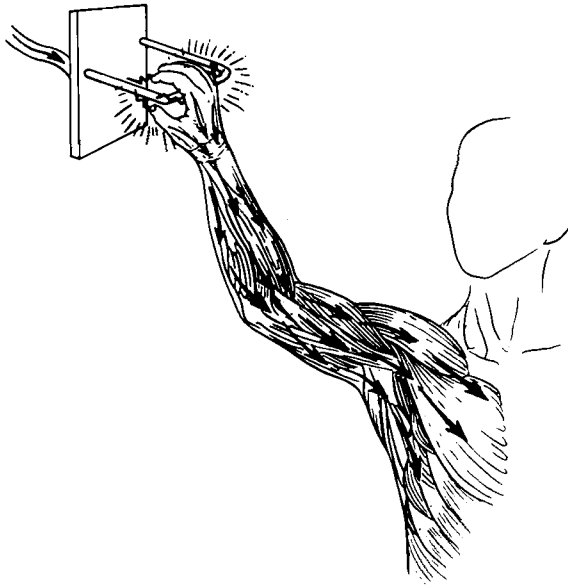
FIG. 1. Illustration of current path through upper extremity during a typical electrical accident. Electric field lines are generally near parallel to the major axis of the skeletal muscle cells.

to the electric field, reaching its greatest magnitude when the major axis of the cell is parallel to the average direction of the electric field.

To illustrate the significance of cell size, a geometrically simple model of an elongated cell, such as the skeletal muscle cell in Fig. 2(a), is analyzed. The cell membrane is modeled as a cylindrical boundary separating two electrical conductors, which represent the intracellular and extracellular fluids. The membrane and the intracellular and extracellular fluids are assumed to be homogeneous and isotropic, and to have electrical properties that are independent of the applied field until membrane breakdown.

Electrical properties of the plasma membrane can be represented by a series of parallel resistors and capacitors (Rall, 1977), as illustrated in Fig. 2(b). This lumped-parameter circuit model of the membrane is combined with the specified resistivities of the intracellular and extracellular media to result in the well-known cable circuit representation. In the presence of an applied uniform field $E(t)$ in the $\hat{z}$ direction, a change in the transmembrane potential will be induced. Following the examples of Sten-Knudsen (1960), Ranck (1963), and Cooper (1984), the cable equations can be used to solve for the spatial distribution of the induced transmembrane potential. Because human skeletal muscle cells may have significant cross-sectional dimensions, this application of the cable model necessitates the use of a boundary condition which accounts for the transmembrane current through the ends of the cell. The induced transmembrane potential distribution will be solved for isolated muscle cells (Fig. 3(a)) and for cells within intact tissue (Fig. 3(b)) exposed to a uniform sinusoidal electric field of amplitude E_o.
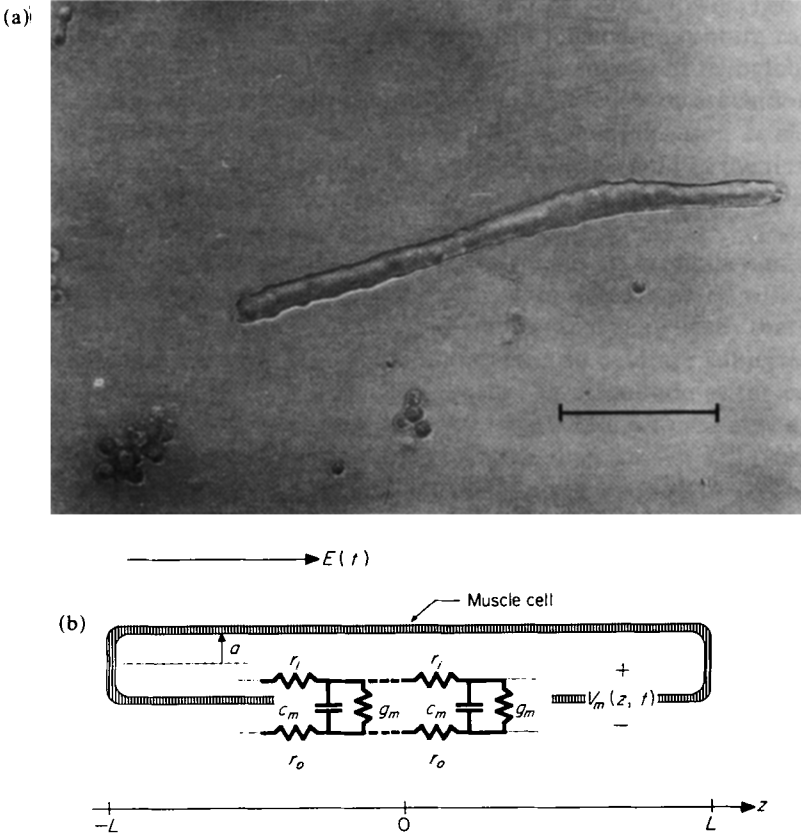
FIG. 2. (a) Intact skeletal muscle cell harvested from rat flexor digitorum brevis muscle. Scale bar is 200 μm. Approximate cell length is 750 μm. (b) Cable circuit model of the cell's electrical properties. Cell length is equal to $2L$; cell radius is a.

Analysis of the circuit model leads to a differential equation for the induced transmembrane potential $v_m(z, t)$:

$$\lambda_m^2 \frac{\partial^2 v_m(z, t)}{\partial z^2} = v_m(z, t) + \tau_m \frac{\partial v_m(z, t)}{\partial t}. \tag{1}$$

The space constant λ_m and the time constant τ_m are given by

$$\lambda_m = \sqrt{\left(\frac{1}{(r_i + r_o)g_m}\right)}, \qquad \tau_m = \frac{c_m}{g_m}, \tag{2}$$

where r_i and r_o are the resistivities (Ω/cm) of the intracellular and extracellular fluids respectively, and c_m and g_m are the capacitance per unit length (F/cm) and the conductance per unit length (mhos/cm) of the membrane respectively. For the case of a single cell in an infinitely extending bath of extracellular fluid, r_o is negligible compared with r_i, since the extracellular space is much greater than the intracellular space. However, when the effects of neighboring cells are considered,
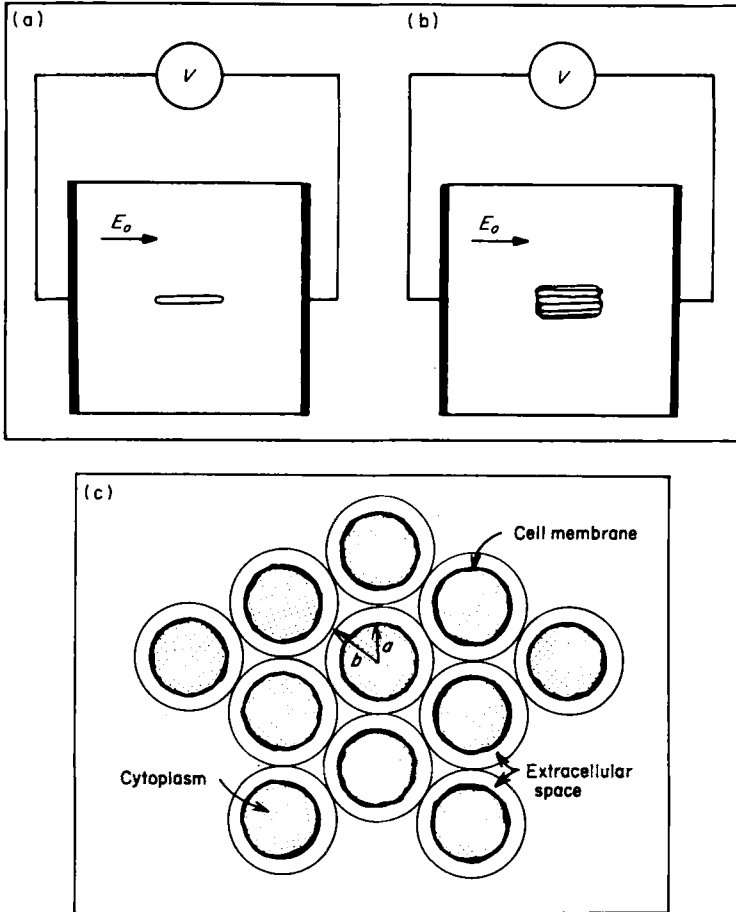
FIG. 3. (a) Isolated muscle cell in a uniform electric field of amplitude E_o driven by an a.c. voltage source of amplitude V. (b) Intact muscle tissue in the same field. (c) Cross section of a hexagonal array of parallel, elongated cells, illustrating the cell radius a and the extracellular fluid radius b.

this approximation is no longer valid. For the isolated cell case, the space constant can be expressed in terms of the cell radius (a), the cell membrane thickness (δ_m), and the conductivities of the intracellular fluid (σ_i) and the membrane (σ_m):

$$\lambda_m = \sqrt{\left(\frac{a\delta_m\sigma_i}{2\sigma_m}\right)}. \tag{3}$$

Because power line a.c. frequencies are of interest in this study, the problem will be solved for the sinusoidal steady state:

$$E(t) = \text{Re}\{E_o\,e^{j\omega t}\} \tag{4}$$

and

$$v_m(z, t) = \text{Re}\{V_m(z)\,e^{j\omega t}\}, \tag{5}$$

where V_m is a complex amplitude and E_o is assumed real. In this case, the differential equation simplifies to

$$\lambda_m^{'2} \frac{d^2 V_m(z)}{dz^2} = V_m(z),$$ (6)

where

$$\lambda_m^{'2} = \frac{\lambda_m^2}{1 + j\omega\tau_m}.$$ (7)

An appropriate solution is

$$V_m(z) = A \sinh(z/\lambda_m'),$$ (8)

where A is a constant to be determined from the boundary conditions. The boundary conditions constraining $V_m(z)$ can be determined from Kirchhoff's voltage law,

$$\frac{d V_m(z)}{dz} = -r_i I_i(z) + r_o I_o(z),$$ (9)

where $I_i(z)$ is the complex amplitude of the total current in the $\hat{z}$ direction inside the cell $(i_i(z, t))$, and $I_o(z)$ is the complex amplitude of the total current in the $\hat{z}$ direction outside the cell $(i_o(z, t))$.

At $z = L$, charge conservation requires

$$G_e \nu_m(L, t) - i_i(L, t) + \frac{d}{dt}[\tau_m G_e \nu_m(L, t) - \tau_i i_i(L, t)] = 0.$$ (10)

The parameter $\tau_i = \varepsilon_i/\sigma_i$ is the charge relaxation time constant reflecting the electrical properties of cytoplasm. The parameter G_e is the conductance of that portion of the membrane which "caps" the end of the cell. It is assumed that the magnitude of the induced transmembrane potential is approximately constant over the entire ends of the cell at $|z| = L$. The error produced by this approximation will be examined later in this section. Taking the time derivative in equation (10) and recognizing that $\omega\tau_i \ll 1$ at 60 Hz leads to the condition

$$I_i(\pm L) = \pm(1 + j\omega\tau_m)G_e V_m(\pm L).$$ (11)

For the isolated cell case, it is assumed that $I_o(z) \gg I_i(z)$ because the extracellular space is much larger than the intracellular space. Therefore, the product $r_o I_o(z)$ can be assumed to be approximately constant, leading to the condition

$$r_o I_o(z) \approx E_o.$$ (12)

The constant A can be determined by substituting the boundary conditions (11) and (12) into equation (9) and evaluating at $z = L$. Thus,

$$V_m(z) = \frac{\lambda_m' E_o}{\cosh(L/\lambda_m')} \frac{\sinh(z/\lambda_m')}{1 + \lambda_m' r_i(1 + j\omega\tau_m)G_e \tanh(L/\lambda_m')}.$$ (13)

With the exception of the term which takes into account the end boundary condition, the form of the solution is consistent with Cooper (1984). In the limit that $L \gg \lambda_m$, the end condition of equation (11) is insignificant and equation (13) gives the same prediction as Cooper. However, when $L \ll \lambda_m$ the end condition is significant. In this limit, it is expected that the intracellular current is approximately independent of position z. That is, the current entering the cytoplasm of a short cell originates mostly at the end of the cell, with negligible current entering through the sides. Thus, the transmembrane potential changes linearly along the length of the cell. This behavior can be readily appreciated from equation (13) by analysis of the $L \ll \lambda_m$ case in the d.c. limit. This predicts that

$$V_m(z) \approx \frac{R_m}{R_i + 2R_m} 2E_o z \quad \text{for } L/\lambda_m \ll 1, \tag{14}$$

where $R_m = 1/G_e$ is the resistance of each of the endcaps of the cell and $R_i = 2Lr_i$ is the resistance of the cytoplasm inside the cell. For $z = L$, $V_m(L)$ is expressed as a fraction of the total voltage across the cell ($2LE_o$) determined by the voltage divider $R_m/(R_i + 2R_m)$. Thus, equation (13) appears to be reasonably valid over the full range of typical skeletal muscle cell sizes.

The error introduced in the assumption of a uniform transmembrane potential ($V_m(\pm L)$) over the total surface of the ends of the cell can be deduced for the worst case of a cell having hemispherical ends. From the solution for a spherical cell ($L = a$) in a uniform field E_o, the magnitude of the potential variation over the hemispherical ends is approximately $\frac{3}{2}E_o a$, leading to an underestimate of the maximum transmembrane potential by about 50% in equation (14). For elongated cells ($L > a$) with spherical ends, the variation will not exceed this amount, and will quickly become negligible compared with the total voltage drop across the cell as the length-to-diameter ratio increases.

For cells within intact tissue subjected to an electric field, the previous analysis can be modified to include the effects of neighboring cells on the induced transmembrane potential. The cells are assumed to be ordered parallel to each other in a hexagonal array as illustrated in Fig. 3(c). To facilitate the comparison of induced transmembrane potential in tissue with the case of isolated cells, the quantity $V_c/2L$ is used as the "source" term, where V_c is the voltage drop across the full length of a cell. For the isolated cell case, $V_c/2L$ is constrained to be E_o in the cable model analysis. For the case of an intact muscle bathed in physiologic fluid with an applied electric field amplitude E_o far away from the muscle, $V_c/2L$ will be greater than E_o by a factor which depends on the degree to which the field is excluded from the intact muscle due to its lower conductivity.

In this tissue model, each cell is surrounded by a volume of extracellular fluid. By symmetry, no current crosses the boundary into the adjacent extracellular region. This conveniently isolates each cell from its neighbors for the purposes of the analysis. Here, the boundaries are approximated by cylinders of radius b as indicated in Fig. 3(c). The total current I_T within each cell's region consists of the intracellular current $I_i(z)$ and the extracellular current $I_o(z)$:

$$I_T = I_i(z) + I_o(z). \tag{15}$$

Longitudinal current in the membrane is ignored because the membrane has negligible cross-sectional area. The cross-sectional area of extracellular space will determine the extracellular resistivity r_o. Generally, for cells that are not on the muscle surface, r_o is not negligible compared with r_i and significantly affects the value of the space constant in equation (2). In addition, the extracellular electric field amplitude between muscle cells is not constant in z. Therefore, the approximation of equation (12) is no longer correct.

The solution form of equation (8) is unchanged but retains a modified coefficient A' to be determined. Kirchhoff's law, equation (9), provides

$$I_T = I_i(z=0)\left(1+\frac{r_i}{r_o}\right)\frac{A'}{r_o\lambda'_m}. \tag{16}$$

By symmetry, the current inside a cell at $z=0$ must be the sum of the current entering from the end (I_e) and from the sides (I_s). I_e is simply $I_i(-L)$, as expressed in equation (11). I_s can be found by

$$I_s = g_m(1+j\omega\tau_m)\int_{-L}^{0} -V_m(z)\,dz = \lambda'_m A' g_m(1+j\omega\tau_m)[\cosh(L/\lambda'_m)-1]. \tag{17}$$

Equations (15)–(17) can be solved for the constant A'. Knowing A', the total currents inside ($I_i(z)$) and outside ($I_o(z)$) the cell can be derived. Integrating either $r_iI_i(z)$ or $r_oI_o(z)$ over the total length of the cell leads to V_c in terms of I_T. Thus

$$V_m(z) = \frac{V_c}{2L}\frac{\lambda'_m(r_o+r_i)/r_i}{\cosh(L/\lambda'_m)}\frac{\sinh(z/\lambda'_m)}{1+\lambda'_m((r_i+r_o)(1+j\omega\tau_m)G_e+r_o/(Lr_i))\tanh(L/\lambda'_m)}. \tag{18}$$

Results

Equations (13) and (18) were used to examine the variation of the transmembrane potential with cell size for the case of isolated cells and variation with both cell size and intracellular spacing for the case of cells within intact muscle. Typical values for the properties of human skeletal muscle cells used in our calculations are (Schanne & Ruiz P.-Ceretti, 1978):

Cell membrane thickness: $\delta_m \approx 10^{-6}$ cm
Cell membrane capacitance: $C_m \approx 3$–$6\ \mu F/cm^2$
Cell membrane conductance: $G_m \approx 1\cdot0$–$2\cdot5\times10^{-4}$ mhos/cm^2
Intracellular fluid permittivity: $\varepsilon_i \approx 80\varepsilon_o$, $\varepsilon_o = 8\cdot854\times10^{-14}$ F/cm
Intracellular fluid conductivity: $\sigma_i \approx 0\cdot01$ mho/cm.

Using average values for human skeletal muscle cells, $\omega\tau_m = \omega C_m/G_m$ is >1 for frequencies greater than approximately 10 Hz. Thus, in the sinusoidal steady state at standard commercial power frequencies (50–60 Hz), $\omega\tau_m$ cannot be neglected and the transmembrane potential and the space constant remain complex quantities. The magnitude of the induced transmembrane potential $V_m(z)$ at 60 Hz was calculated from equation (13) for isolated skeletal muscle cells of several arbitrary lengths with a constant radius 100 μm. The results are plotted in Fig. 4(a) for cells of length
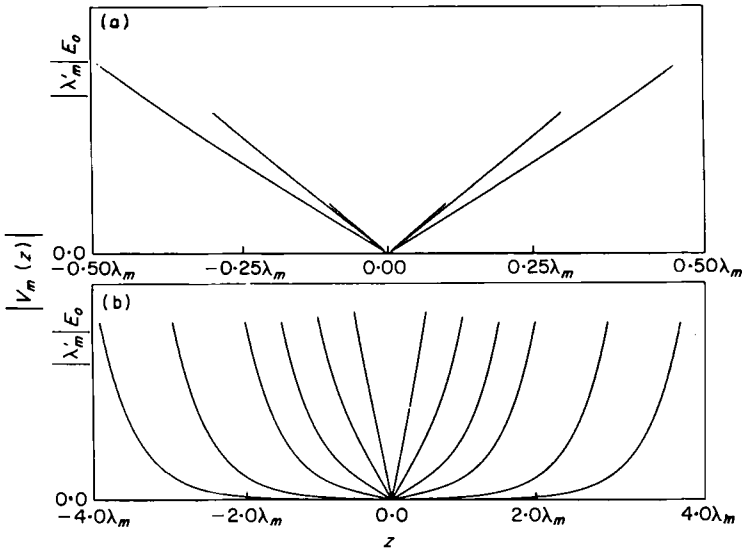
FIG. 4. Plot of the magnitude of $V_m(z)$ at 60 Hz against position on the cell of length $2L$ for radius 100 μm, and (a) for cell lengths $0.2\lambda_m$, $0.6\lambda_m$, λ_m, and (b) for longer cell lengths λ_m, $2.0\lambda_m$, $3.0\lambda_m$, $4.0\lambda_m$, $6.0\lambda_m$ and $8.0\lambda_m$, The cells are centered on the z-axis.

$0.2\lambda_m$, $0.6\lambda_m$, λ_m, and in Fig. 4(b) for cells of length $1.0\lambda_m$, $2.0\lambda_m$, $3.0\lambda_m$, $4.0\lambda_m$, $6.0\lambda_m$, and $8.0\lambda_m$.

For cells that are short compared with their space constant, the induced transmembrane potential varies linearly with z, is constrained by symmetry to be zero at the origin and reaches a maximum at the cell ends. For longer cells, the transmembrane potential has a more exponential dependence, which indicates that the imposed transmembrane current is disproportionately concentrated toward the ends. Because the maximum imposed transmembrane potential magnitude (V_{max}) occurs at the ends of the cell, we define

$$V_{max} = |V_m(-L)| = |V_m(L)|. \tag{19}$$

The extent to which cell structure leads to intramembrane field intensification can be appreciated from equation (13). If the cell membrane conductivity were equal to that of the cytoplasm or extracellular fluid, then V_{max} would equal $E_o\delta_m$. If the cell membrane were perfectly insulating, V_{max} would equal E_oL. For muscle cells with characteristic membrane properties which are short enough that the resistance of the membrane is infinite compared with the cytoplasm, V_{max} is equal to E_oL. For longer cells, the maximum value of V_{max} reaches $E_o|\lambda'_m|$, because the space constant λ'_m reflects the value of the membrane conductivity relative to the conductivity of the intracellular and extracellular fluid.

In the sinusoidal steady state, V_{max} does not increase monotonically with cell length, as expected for the d.c. case. Instead, in the L co-ordinate, V_{max} behaves as a heavily damped oscillator superimposed on the d.c. solution. It reaches its first
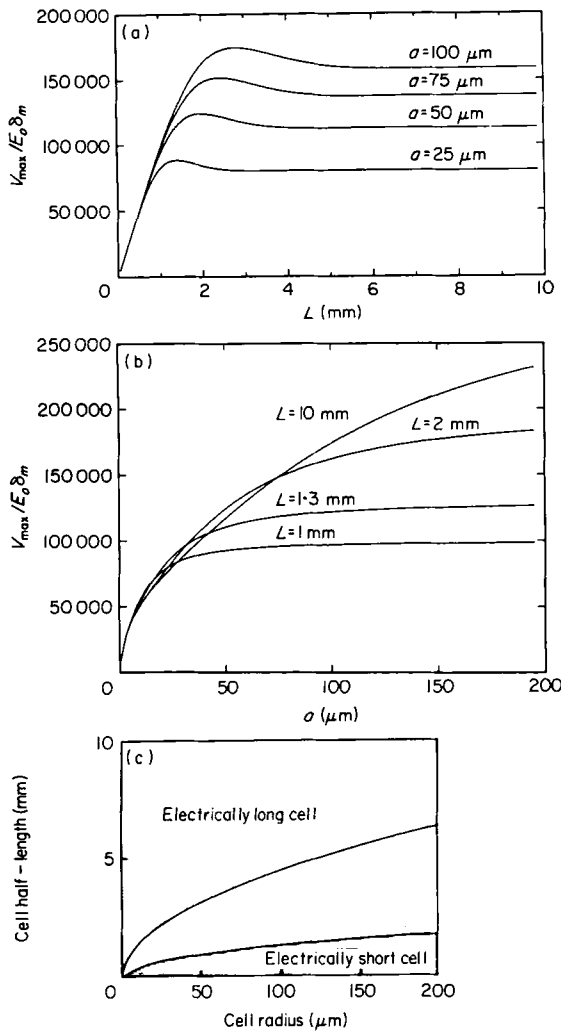
FIG. 5. (a) Absolute magnitude of the induced transmembrane potential at the end of the muscle cell (V_{max}) increases with cell length, reaches a frequency-dependent maximum value, then decreases to a plateau limiting value of $|\lambda'_m|E_o$ for very long cells. (b) Maximum transmembrane potential increases with cell radius, reaching the maximum value predicted for electrically short cells (equation (14)). (c) Classification of the electrical properties of cells on the basis of their dimensions.

and only significant maximum at

$$L \approx \frac{\sqrt{2}\,\pi\lambda_m}{2\sqrt{-1+(1+\omega^2\tau_m^2)^{0\cdot5}}}, \tag{20}$$

which is determined by the frequency, cell radius and the electrical properties of the membrane. Then V_{max} decreases to a plateau of $|\lambda'_m|E_o$. This behavior is illustrated

illustrated in Fig. 5(a). At 60 Hz the maximum occurs at $L \approx 0.86\lambda_m$ and $|\lambda'_m|E_o$ is approximately one-third $\lambda_m E_o$.

For long cells V_{max} is strongly dependent on cell radius. For short cells ($L \ll \lambda_m$), V_{max} is independent of cell radius. However, as the radius increases, the length of the cell over which membrane resistance governs the intracellular current increases. This added length allows a higher potential (V_{max}) to be imposed across the ends of the cell.

These results suggest a classification of cells into 3 groups, depending on their electrical properties. The electrically long cells, having large length-to-radius ratios, have a V_{max} which is independent of length, but increases with radius. The electrically short cells, having small length-to-radius ratios, have a V_{max} which is independent of radius, but increases with length. Cells having dimensions between these two limits have a V_{max} which increases with both length and radius. Figure 5(c) illustrates approximate boundaries for these classifications.

The effect of adjacent cells is fundamentally to limit the extracellular space available to each cell. This results in an increase in the maximum transmembrane potential for any given cell length and radius. The smaller the extracellular space, the greater the increase. This is illustrated in Fig. 6 where V_{max} is plotted as a function of b/a for a cell of length 10 mm ($L = 5$ mm) and radius 50 μm. This result
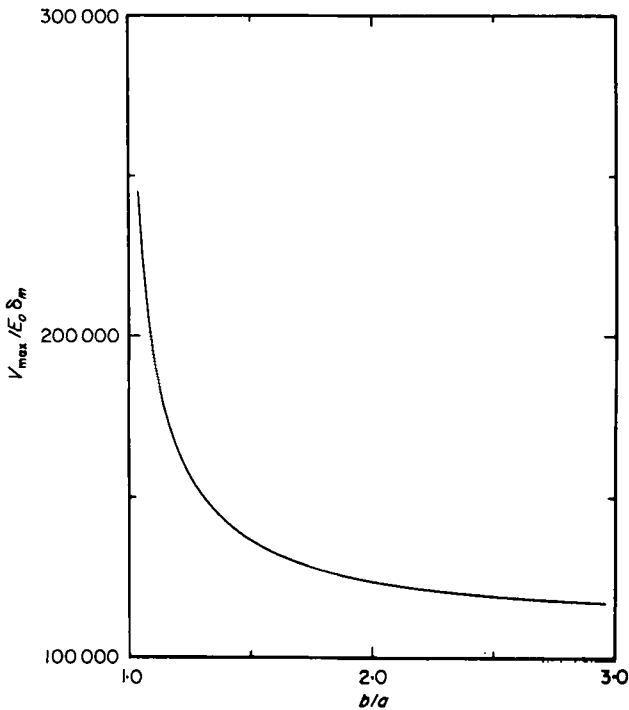

FIG. 6. Maximum transmembrane potential (V_{max}) for an array of cells ($L = 5$ mm, $a = 50$ μm) increases with a decrease in the extracellular spacing, starting (for $b/a \gg 1$) at that predicted for isolated cells, and ending (for $b/a \approx 1$) at that predicted by equation (21).

can be readily interpreted. When a cell is isolated in extracellular fluid, the low resistance of the extracellular fluid acts to short out the voltage drop across the length of the cell. In other words, the current tends to flow around rather than through the cell. When other cells are brought in close proximity, the resistance of the extracellular path increases and more current will flow end-to-end through the cell. This results in a greater transmembrane potential at the ends of the cell. In addition, because the space constant λ'_m is decreased by an increased r_o, the induced transmembrane potential is more confined near the ends of the cells.

As the ratio b/a becomes large, that is, as r_o becomes small, V_{max} approaches that predicted for an isolated cell of the same dimensions. As the ratio b/a approaches unity, that is, as r_o approaches infinity, the cell appears to be a lumped three-element voltage divider. Thus, in the d.c. case,

$$V_{max} \approx \frac{V_c}{2} \frac{1/(2Lr_i)}{G_e/2 + 1/(2Lr_i)}, \quad \text{when } b/a \approx 1. \tag{21}$$

The voltage divider does not depend on cell radius, and is in fact the same voltage divider relationship derived for isolated cells of short length to radius ratios (equation (14)). This is not surprising since a bundle of cells with no extracellular space ($r_o = \infty$) will behave like a single cell of the same length but greater radius. Thus, the response can be described by the isolated cell model, with $E_o = V_c/2L$.

Discussion

The previous analysis shows that, in the presence of an imposed a.c. electric field, cells of a specific frequency-dependent size oriented parallel to the field experience a higher transmembrane potential than shorter or longer cells or cells oriented perpendicular to the field. Also, for cells not electrically short, those of large radius can experience significantly higher transmembrane potentials than cell types of smaller radius. That this larger potential causes an increased susceptibility to cell membrane breakdown and rupture is well established.

Two types of membrane breakdown due to an applied electric field have been experimentally demonstrated (see Powell & Weaver, 1986). The first, membrane rupture, has been shown to occur in bilayer lipid membranes for transmembrane potentials exceeding 200–500 mV applied for $>10^{-4}$ sec. A second type of membrane breakdown, a non-destructive reversible breakdown, has been shown to occur in bilayer lipid membranes whenever transmembrane potentials of between 500 and 1000 mV are applied for shorter times ($<10^{-5}$ sec). This type of breakdown manifests itself in a dramatic drop in the electrical resistance of the membrane, but the membrane survives. For biological membranes, the reported voltage thresholds for electric breakdown are generally higher, at about 1 V (Benz et al., 1979).

Many theories have been proposed regarding the mechanism by which cell membrane breakdown occurs. These theories examine the mechanical, electrical, and chemical factors which cause pores in fluids and membranes (both artificial and biological) to form, and once formed, to expand or contract. In a classic paper by Taylor & Michael (1973), it was suggested that axisymmetric holes in thin sheets

of fluid where surface tension forces predominate will expand if their initial radii are larger than the thickness of the sheet, while holes with radii smaller than this thickness will close. This is due to the action of the interfacial tension, which acts to reduce surface area.

A similar approach was used by Weaver (Weaver & Mintzer, 1981; Powell & Weaver, 1986). His theory expands on the work of Litster (1975), who introduced the idea of the Brownian motion of molecules of the surrounding media causing pores to form in bilayer membranes. These pores are restrained by the mechanical forces at a pore's edge. The energy ΔE needed to create a pore of radius r is the increase in energy associated with the creation of the edge of the pore less the energy of the eliminated surface area:

$$\Delta E = 2\pi\gamma r - \pi\Gamma r^2. \tag{22}$$

Γ is the bifacial energy per unit area of the membrane and γ is the strain energy per unit length of the membrane pore edge. Weaver added a term to this energy equation to include electrostatic energy effects which are associated with a transmembrane potential V_m:

$$\Delta E = 2\pi\gamma r - \pi r^2(\Gamma + \alpha V_m^2), \tag{23}$$

where α is a positive parameter dependent on the permittivities of the membrane and the intracellular and extracellular fluids and the membrane thickness δ_m. Thus, V_m tends to decrease the stability of the membrane against thermal fluctuations by decreasing the amount of energy required to form a pore. An applied V_m also lowers the critical pore radius beyond which mechanical forces at the pore's edge cannot restrain the pore from expanding until cell rupture.

It has been shown that the presence of neighboring cells in a tissue prevents current from being diverted around a given cell, and instead forces more current to flow through the ends of the cell. This effect is more pronounced the closer the neighboring cells are located. The same idea can be applied to a study of the effects of various other cellular environments on the imposed transmembrane potential and thus the vulnerabilities of various cells to breakdown.

It seems reasonable that cells at the very edge of an intact muscle would experience a lower transmembrane potential than those in the interior since cells on the edge are exposed to the higher conducting fascial planes which short out the potential. The situation for cells adjacent to cortical bone is exactly the opposite. The cortical bone, being less hydrated than extracellular fluid, is far more resistive. As a result, cells next to bone would experience a higher transmembrane potential due to a greater amount of current flowing through the cell membranes. Thus, it seems reasonable that the cells closest to the bone are more likely to be ruptured by non-thermal electrical forces than the cells adjacent to the fascial plane.

These results suggest a pattern of injury which correlates strongly with clinical observation. When the current path includes an upper extremity, victims of electrical trauma have been found to develop a characteristic pattern of tissue injury. In tissue locations far enough away from the surface contact points so that the local temperature is unaffected by intense skin heating, the muscle injury has been observed

to be the most severe around bone (Baxter, 1970; Hunt *et al.*, 1980) and in the cental core of the muscle (Zelt *et al.*, 1986).

Conclusions

We have applied the cable model to the cases of a single elongated cylindrical cell and of an array of such cells to obtain a physically reasonable prediction of the induced transmembrane potential along the length of the cell. The analysis indicates that cell size is very important in determining the magnitude of the induced transmembrane potential experienced by cells in an imposed electric field.

Once sinusoidal steady-state conditions are reached, the induced transmembrane potential is not a simple monotonic function of cell length. Rather, there is an optimum cell length-to-radius ratio which brings about the maximum induced transmembrane potential. If the radius is held relatively constant, increases in cell length beyond the optimum bring about a decrease in the induced transmembrane potential. In addition, small changes in cell length centered about the length of maximum transmembrane potential can lead to significant changes in the induced transmembrane potential. Because the probability of rupture is proportional to the square of the transmembrane potential, the susceptibility to rupture is strongly cell-size dependent.

Because muscle and nerve cells are much larger than other cell types and thus generally develop larger transmembrane potentials in an applied field, they should be more vulnerable to injury. This prediction is consistent with clinical observation. In addition, it has been shown that the transmembrane potential at the ends of a cell in a tissue increases with a decrease in extracellular space due to the decrease in extracellular resistivity. This helps explain the clinical observation that the central core of a muscle and muscle adjacent to bone seem the most susceptible to damage.

REFERENCES

BAXTER, C. R. (1970). *Surg. Clin. North Am.* **50**, 1401.
BENZ, R., BECKERS, F. & ZIMMERMAN, U. (1979). *J. membr. Biol.* **48**, 181.
BUTLER, E. & GANT, T. (1977). *Am. J. Surg.* **134**, 95.
COOPER, M. S. (1984). *J. theor. Biol.* **111**, 123.
FARRELL, D. F. & STARR, A. (1968). *Neurology* **18**, 601.
HUNT, J. L., SATO, R. M. & BAXTER, C. R. (1980). *Arch. Surg.* **115**, 434.
JAFFE, R. H. (1928). *Arch. Path.* **5**, 837.
LEE, R. C. & KOLODNEY, M. S. (1987). *Plast. Reconstr. Surg.* **80**, 672.
LITSTER, J. D. (1975). *Phys. Lett.* **53**(A), 193.
MORITZ, A. R. & HENRIQUES, F. C. (1947). *Am. J. Path.* **23**, 695.
MOUSSA, N. A., MCGRATH, J. J., CRAVALHO, E. G. & ASIMACOPOULOS, P. J. (1979). *J. Biomech. Eng.* **101**, 213.
POWELL, K. T. & WEAVER, J. C. (1986). *Bioelectrochem. Bioenerg.* **15**, 211.
RALL, W. (1977). In: *Handbook of Physiology—The Nervous System.* Vol. 1. Bethesda, Maryland: American Physiological Society.
RANCK, J. B. (1963). *Expl Neurol.* **7**, 153.
ROBSON, M. C., MURPHY, R. C. & HEGGERS, J. P. (1983). *Plast. Reconstr. Surg.* **73**, 437.
SANCES, A., LARSON, S. J., MYKLEBUST, J. & CUSICK, J. F. (1979). *Surg. Gynec. Obstet.* **149**, 97.
SCHANNE, O. F. & RUIZ, P.-CERETTI, E. (1978). *Impedance Measurements in Biological Cells.* New York: John Wiley.

STEN-KNUDSEN, O. (1960). *J. Physiol.* **151**, 363.

TAYLOR, G. I. & MICHAEL, D. H. (1973). *J. Fluid Mech.* **58**, pt. 4, 625.

TRANCHINA, D. & NICHOLSON, C. (1986). *J. Biophys. Soc.* **50**, 1139.

WEAVER, J. C. & MINTZER, P. A. (1981). *Phys. Lett.* **86**(A), 57.

ZELT, R. G., BALLARD, P. A., HEROUX, P. & DANIEL, R. K. (1986). *Proc. 55th Ann. Sci. Mtg. Am. Soc. Plastic Reconstr. Surg.* **9**, 222.